PHYSICAL REVIEW B **68**, 140301(R) (2003)

Local thermal expansion in copper: Extended x-ray-absorption fine-structure measurements and path-integral Monte Carlo calculations

S. a Beccara, G. Dalba, P. Fornasini,* R. Grisenti, F. Pederiva, and A. Sanson
Istituto Nazionale per la Fisica della Materia and Dipartimento di Fisica, Università di Trento, I-38050 Povo (Trento), Italy

D. Diop
Faculté des Sciences et Techniques, Université Cheikh Anta Diop, Dakar, Senegal

F. Rocca
IFN, Istituto di Fotonica e Nanotecnologie del Consiglio Nazionale delle Ricerche, Sezione CeFSA di Trento, 38050 Povo (Trento), Italy
(Received 29 April 2003; revised manuscript received 14 July 2003; published 2 October 2003)

A combined approach has been used to study thermal effects on the extended x-ray absorption fine-structure (EXAFS) of copper between 4 and 500 K. A phenomenological data analysis shows that the thermal expansions measured from the first and third cumulants significantly differ between each other and from the crystallographic thermal expansion. Path-integral Monte Carlo calculations of EXAFS cumulants have been performed, using a many-body potential. The good reproduction of experimental values validates the phenomenological analysis and opens more perspectives for applications to more complex systems. It is shown that the reproduction of EXAFS parameters allows for a test of the interaction potentials with regard to anharmonicity.

DOI: 10.1103/PhysRevB.68.140301 PACS number(s): 61.10.Ht, 65.40.De

The possibility of extracting original information on local thermal expansion and correlation of atomic motion in crystals from extended x-ray-absorption fine-structure (EXAFS) has been emphasized by many recent works.[1–6] The interpretation of thermal effects over an entire EXAFS spectrum, including multiple-scattering effects, requires to perform configurational averages over reliable samples of statistical ensembles.[7] Actually, data analyses generally rely on several assumptions and approximations. In particular, when only the nearest-neighbor EXAFS signal is considered, a phenomenological analysis based on the distribution of interatomic distances is usually done, which, for moderate disorder, can be further simplified by a parametrization in terms of cumulants.[8,9] The distribution of distances has been related to a mean-force one-dimensional anharmonic potential $V_e(r)$.[1,10,11] Quantitative relations between EXAFS cumulants and force constants of $V_e(r)$ have been obtained on the basis of a quantum statistical perturbative approach.[12,13]

A weakness of the widespread one-dimensional model lies in the nontrivial relation between EXAFS cumulants and mean-force potential $V_e(r)$ on the one hand, and the physical properties of a solid on the other, as evidenced by recent experiments on crystals.[2,5,6] First, the average nearest-neighbor distance and its thermal expansion, measured by the first cumulant, are larger than the distance between average positions and the corresponding crystallographic thermal expansion (CTE), due to atomic vibrations perpendicular to the bond direction. Second, different information concerning thermal expansion is carried by the first and third cumulants, contrary to the expectations of the one-dimensional model.[10,12] In the case of germanium,[5] the thermal expansion measured from the third cumulant satisfactorily reproduced the CTE, so that the first-cumulant thermal expansion could be considered as the sum of two effects: the asymmetry of $V_e(r)$ (measured by the third cumulant) and its positive shift induced by atomic vibrations perpendicular to the bond.[9] In the case of AgI, on the contrary, neither the first nor the third cumulants satisfactorily reproduced the CTE;[2] here, a negative shift of the mean-force potential was observed, reproduced by molecular-dynamics (MD) simulations[2] and attributed to the high mobility of Ag cations.[14] Not only cannot thus the mean-force potential $V_e(r)$ be confused with a pair interaction potential, but also a simple interpretation of general validity of its position and shape seems impossible.

In spite of the recent advances in EXAFS interpretation,[15] thermal effects still represent in many instances a challenging problem; a deeper insight would enhance the accuracy, avoid misinterpretations, and exploit the ultimate potentialities of EXAFS-based structural studies. To this aim, careful measurements on systems of different structural and dynamical complexity are necessary. Besides, the calculation of thermal parameters by means of theoretical techniques, independent of experimental data, is important in order to validate the phenomenological data analysis procedures.

A simple connection between EXAFS cumulants and pair interaction potential has been sought for a cluster of atoms in Ref. 16. Full quantum-mechanical calculations, based on perturbation theory, have been performed for a one-dimensional chain[17] and for monatomic fcc systems.[18] To overcome the limitations of perturbative treatments, an approach based on path-integral techniques has been recently proposed.[19] The EXAFS cumulants have been calculated for the Br_2 molecule and for solid krypton and nickel[20] within the path-integral framework using the effective potential approximation.[21]

To deal with systems with many degrees of freedom, numerical simulation techniques are particularly appealing. Besides allowing for the use of realistic potentials, they deliver sets of configurations distributed according to statistical ensembles. Path-integral Monte Carlo[22] (PIMC) allows to study equilibrium properties taking into account both anharmonic-

ity and low-temperature quantum effects. PIMC is based on the sampling of the thermal density matrix after its factorization into the product of P matrices with effective temperature P times higher, corresponding to P copies of the system *(slices)*. The resulting probability distribution is sampled by means of appropriate generalized Metropolis algorithms. The PIMC algorithm is exact in the limit $P \to \infty$. The reliability of PIMC results only depends on the validity of the Born-Oppenheimer approximation and on the accuracy of the modeling crystal potential. PIMC can be exploited to construct sets of atomic configurations. Relevant physical observables, such as cumulants of distance distributions, can be directly obtained from configurational averages. Besides, the set of atomic configurations can be used as input for EXAFS simulations taking into account multiple-scattering paths.

In this Rapid Communication, we present a joint experimental and theoretical study of the EXAFS of copper in the temperature range from 4 to 500 K. The contribution of the first coordination shell has been analyzed by a phenomenological procedure, in order to clarify the relation between first and third EXAFS cumulants and the CTE. In parallel, a PIMC simulation has been performed.

Since the available EXAFS data on copper were limited to a few temperatures,[23–26] measurements have been made at the BM08 (Gilda) beamline of ESRF (European Synchrotron Radiation Facility), Grenoble, using a (311) silicon crystal monochromator. The sample was a copper foil of 99.97% purity, 5 μm thickness, light tested, and annealed at 973 K (purchased from Goodfellow Ltd). EXAFS signals were extracted from experimental spectra according to well established procedures.[5,27] The first-shell contribution to EXAFS at different temperatures, obtained through Fourier filtering, was analyzed by the *ratio method*, using the 4-K spectra as reference.[8] The results of the analysis were the relative values of the first four cumulants $\delta C_i = C_i(T) - C_i(4\ \mathrm{K})$ of an *effective* distribution $P(r,\lambda) = \rho(r)\exp(-2r/\lambda)/r^2$.[9] The error bars were evaluated by reasonably varying the parameters of the analysis procedure and cross comparing the results from different files measured at the same temperature. The difference between cumulants C_i of the effective distribution and C_i^* of the real distribution $\rho(r)$ was significant only for the first one:[5,9]

$$C_1^* \simeq C_1 + (2C_2/C_1)(1 + C_1/\lambda). \tag{1}$$

Three different values of λ (6, 9, and 12 Å) were used in Eq. (1), to compensate for neglecting the dependence of λ on the photoelectron wave number.

PIMC simulations were performed on a system of 108 atoms with periodic boundary conditions. The cell parameter was held fixed at each temperature according to available crystallographic data.[28] This choice allows to avoid the possible bias on the crystallographic thermal expansion due to the choice of the potential, thus permitting to study *local* phenomena with higher accuracy. Besides, it considerably reduces the computational load. The number of slices was varied with temperature: 8, 64, and 128 slices were found to guarantee a satisfactory convergence for $T > 200$ K, $40 < T < 200$ K, and $T < 40$ K, respectively. The sampling method

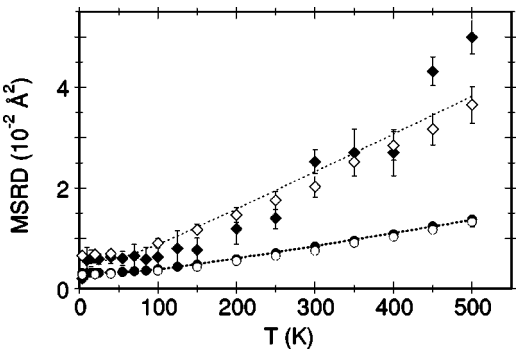

FIG. 1. Parallel and perpendicular MSRD for the first shell of copper: experimental EXAFS results (full circles and diamonds), correlated Einstein models (dashed lines), and PIMC results (open circles and diamonds).

employed a combination of a single-slice and a multiple-slice move. In the single-slice move, one or more atoms belonging to the same slice are displaced. In the multiple-slice move, atoms belonging to more than one slice are displaced at the same time. The single-slice move was performed according to the force-bias method, in order to improve acceptance.[29] The multiple-slice move was performed by means of the Lévy bridge construction, in a recursive fashion.[22] This move displaces $2^n - 1$ atoms in neighboring slices, exactly sampling the distribution of a system of harmonic oscillators. The number of atoms displaced, i.e., the sampling depth, was held constant. A many-body potential of the tight-binding family[30] (SMA-TB) was chosen. The total energy is a sum over all atoms i of a many-body attractive term

$$E_b^i = -\left[\sum_{j \neq i} \xi^2 e^{-2q(r_{ij}/r_0 - 1)}\right]^{1/2} \tag{2}$$

and a two-body Born-Mayer repulsive term

$$E_r^i = A \sum_{j > i} e^{-p(r_{ij}/r_0 - 1)}. \tag{3}$$

This potential had been previously used by Edwards *et al.* for a MD calculation of the EXAFS cumulants of copper, obtaining a good agreement with available experimental data at high temperature.[31] The same parameter values have been chosen in the present work, to allow a reasonable comparison between MD and PIMC.

It is convenient to begin the discussion of results from the second cumulant C_2^*, corresponding, to a very good approximation, to the parallel projection $\langle \Delta u_{||}^2 \rangle$ of the mean-square relative displacement (MSRD):[9]

$$\langle \Delta u^2 \rangle = \langle (\vec{u}_j - \vec{u}_0)^2 \rangle = \langle \Delta u_{||}^2 \rangle + \langle \Delta u_{\perp}^2 \rangle. \tag{4}$$

Absolute values of the second cumulant C_2^* (full circles in Fig. 1) were estimated by fitting Debye and Einstein correlated models to the experimental δC_2^* data. The Einstein model gave slightly higher values, 3% at 4 K, less than 1% at 500 K. The Debye temperature was 327 K, in good agreement with previous EXAFS results and with specific-heat

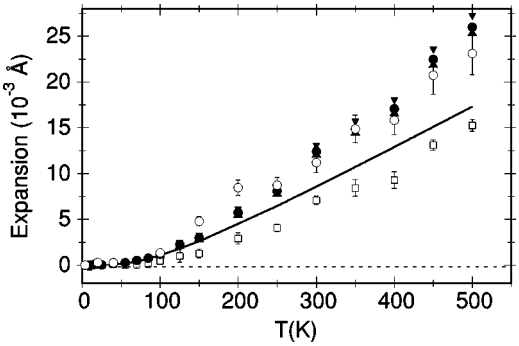

FIG. 2. Temperature dependence of the first cumulants for the first shell of copper: δC_1 of the effective EXAFS distribution (open squares and error bars); δC_1^* of the real distribution, from experiment for $\lambda = 6$, 9, and 12 Å (down triangles, full circles, and up triangles, respectively), and from PIMC (open circles). Continuous line is crystallographic expansion δR.

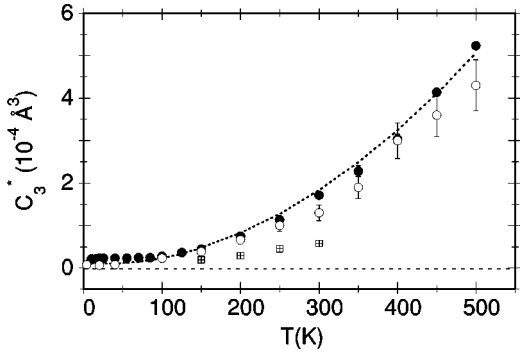

FIG. 3. Third cumulant C_3^* for the Cu first shell from EXAFS (full circles) and PIMC calculations with a many-body potential (open circles) and a two-body potential (crossed squares). The dashed line is the best-fitting model based on the quantum perturbative anharmonic treatment of Refs. 12 and 13.

measurements (315–343 K). The Einstein frequency was 4.99 THz, corresponding to a second-order force constant $k_0 = 3.24$ eV/Å^2 for the potential $V_e(r)$. The parallel MSRD $\langle \Delta u_{||}^2 \rangle$, calculated by PIMC as $\langle (r - \langle r \rangle)^2 \rangle$, is shown by open circles in Fig. 1. The low-temperature quantum effect of zero-point energy is well reproduced, contrary to classical MD simulations.[31] PIMC values are lower than the Debye model (7% and 1% at 4 and 500 K, respectively), the discrepancy being possibly due to the inadequacy of the Debye model at low temperatures.

In Fig. 2, the temperature dependence of the first EXAFS cumulants (full circles) is compared with the CTE from Ref. 28 (continuous line). The first cumulant C_1^* of the real distribution of distances is to first order connected to the crystallographic distance R through[5,9]

$$C_1^* = R + \langle \Delta u_\perp^2 \rangle / 2R. \tag{5}$$

Since the perpendicular MSRD $\langle \Delta u_\perp^2 \rangle$ grows with temperature, the EXAFS thermal expansion δC_1^* is larger than the CTE δR. The experimental behavior (full circles) is well reproduced by the $\langle r \rangle$ values calculated by PIMC (open circles). Absolute values of $\langle \Delta u_\perp^2 \rangle$ were calculated, as in Ref. 5, by fitting an Einstein model to the relative values $2R(\delta C_1^* - \delta R)$. The perpendicular MSRD values so obtained are shown in Fig. 1 (full diamonds) and compared with the values calculated by PIMC as $\langle \Delta u^2 \rangle - \langle \Delta u_{||}^2 \rangle$ (open diamonds). The ratio $\gamma = \langle \Delta u_\perp^2 \rangle / \langle \Delta u_{||}^2 \rangle$ calculated from PIMC is about 2.7 at high temperature. At high temperature, γ should be 2 for a perfect parallel-perpendicular isotropy; a value 6 was experimentally found for the first shell of germanium.[5]

Let us consider the third cumulant (Fig. 3). Absolute values of C_3^* were obtained by fitting the temperature dependence of the experimental values δC_3^* to the quantum analytical expression of Refs. 12 and 13. The third-order force constant of $V_e(r)$ was estimated $k_3 = -1.53$ eV/Å^3, and was then used to find the thermal expansion $a = -3k_3 C_2^*/k_0$ solely due to the asymmetry of the $V_e(r)$ potential.[12] A zero-point value $a_0 = 4.5 \times 10^{-3}$ Å was found (it was 3 $\times 10^{-3}$ Å for germanium[5]). The temperature dependence δa is compared with the CTE δR in Fig. 4. The slope of δa is smaller than the slope of δR, indicating that the crystallographic thermal expansion is not reproduced by the anharmonicity of the potential $V_e(r)$. The difference between δC_1^* and δR, due to thermal vibrations perpendicular to the bond direction, is connected to a rigid positive shift of the effective potential.[9] The difference between δR and δa suggests the presence of a further positive shift. The relationship between anharmonicity of the crystal potential and asymmetry of $V_e(r)$ is thus far from trivial even for simple crystals such as copper; the behavior found for germanium, $\delta a = \delta R$,[5] was a peculiar coincidence, and cannot be generalized. The third cumulant calculated by PIMC as $\langle (r - \langle r \rangle)^3 \rangle$ is in satisfactory agreement with experimental data, including the finite value extrapolated at $T = 0$ K (open circles in Fig. 3). The sensitivity of PIMC results to the choice of the interaction potential was checked by using a simpler two-body potential[32] instead of the many-body potential. While the first and second cumulants were again satisfactorily reproduced, the third cumulant was dramatically smaller than the experimental values (Fig. 3, crossed squares).

In conclusion, accurate temperature-dependent measure-

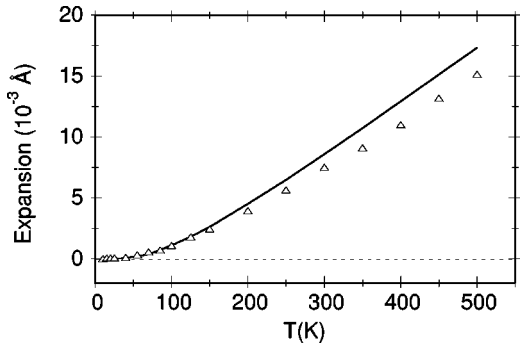

FIG. 4. Temperature dependence δa of the nearest-neighbor distance in copper, measured by the model of Frenkel and Rehr (Ref. 12) based on the third cumulant (triangles). The continuous line is the crystallographic thermal expansion δR.

ments on copper have shown that EXAFS gives different and complementary information on thermal expansion with respect to Bragg diffraction. The first-cumulant difference can be exploited to gain original information on atomic motion perpendicular to the bond direction. The third-cumulant difference indicates that the anharmonicity of the mean-force potential has no trivial interpretation, and the one-dimensional model should be cautiously used when interpreting EXAFS results for systems with many degrees of freedom.

The EXAFS cumulants, calculated by PIMC, were in good agreement with the experimental values. This result, besides representing a validation of the phenomenological first-shell data analysis, opens more perspectives for studying vibrational dynamics not only in crystalline solids (including outer coordination shells) but also in noncrystalline systems. Moreover, the possibility has been demonstrated of offering an additive test of interatomic potentials by means of the reproduction of EXAFS thermal parameters.

The authors are grateful to the staff of the BM08-Gilda beamline at ESRF for experimental assistance and to D. M. Ceperley and G. Garberoglio for useful discussions. INFM financial support (Project No. BM08-01-290) is acknowledged.

*Email address: fornasin@science.unitn.it

[1] J.M. Tranquada and R. Ingalls, Phys. Rev. B **28**, 3520 (1983).
[2] G. Dalba, P. Fornasini, R. Gotter, and F. Rocca, Phys. Rev. B **52**, 149 (1995).
[3] T. Yokoyama, T. Ohta, and H. Sato, Phys. Rev. B **55**, 11 320 (1997).
[4] O. Kamishima, T. Ishii, H. Maeda, and S. Kashino, Solid State Commun. **103**, 141 (1997).
[5] G. Dalba, P. Fornasini, R. Grisenti, and J. Purans, Phys. Rev. Lett. **82**, 4240 (1999).
[6] S. a Beccara, G. Dalba, P. Fornasini, R. Grisenti, A. Sanson, and F. Rocca, Phys. Rev. Lett. **89**, 025503 (2002).
[7] M. Benfatto, C.R. Natoli, and A. Filipponi, Phys. Rev. B **40**, 9626 (1989).
[8] G. Bunker, Nucl. Instrum. Methods Phys. Res. **207**, 437 (1983).
[9] P. Fornasini, F. Monti, and A. Sanson, J. Synchrotron Radiat. **8**, 1214 (2001).
[10] L. Tröger, T. Yokoyama, D. Arvanitis, T. Lederer, M. Tischer, and K. Baberschke, Phys. Rev. **49**, 888 (1994).
[11] E.A. Stern, J. Phys. IV **7**, 137 (1997).
[12] A.I. Frenkel and J.J. Rehr, Phys. Rev. B **48**, 585 (1993).
[13] T. Yokoyama, J. Synchrotron Radiat. **6**, 323 (1999).
[14] T. Ishii, J. Phys. Soc. Jpn. **70**, 159 (2001).
[15] J.J. Rehr and R.C. Albers, Rev. Mod. Phys. **72**, 621 (2000).
[16] N. Van Hung and J.J. Rehr, Phys. Rev. B **56**, 43 (1997).
[17] T. Fujikawa and T. Miyanaga, J. Phys. Soc. Jpn. **62**, 4108 (1993).
[18] H. Katsumata, T. Miyanaga, T. Yokoyama, T. Fujikawa, and T. Ohta, J. Synchrotron Radiat. **8**, 226 (2001).
[19] T. Fujikawa, T. Miyanaga, and T. Suzuki, J. Phys. Soc. Jpn. **66**, 2897 (1997).
[20] T. Yokoyama, Phys. Rev. B **57**, 3423 (1998).
[21] A. Cuccoli, R. Giachetti, V. Tognetti, R. Vaia, and P. Verrucchi, J. Phys.: Condens. Matter **7**, 7891 (1995).
[22] D.M. Ceperley, Rev. Mod. Phys. **67**, 279 (1995).
[23] W. Böhmer and P. Rabe, J. Phys. C **12**, 2465 (1979).
[24] R.B. Greegor and F.W. Lytle, Phys. Rev. B **20**, 4902 (1979).
[25] E.A. Stern, B.A. Bunker, and S.M. Heald, Phys. Rev. B **21**, 5521 (1980).
[26] T. Yokoyama, T. Satsukawa, and T. Ohta, Jpn. J. Appl. Phys., Part 1 **28**, 1905 (1989).
[27] G. Dalba, P. Fornasini, and F. Rocca, Phys. Rev. B **47**, 8502 (1993).
[28] Y.S. Touloukian, R.K. Kirby, R.E. Taylor, and P.D. Desai, *Thermophysical Properties of Matter*, (Plenum, New York, 1977), Vol. 13.
[29] M.P. Allen and D.J. Tidesley, *Computer Simulation of Liquids* (Oxford University Press, Oxford, 1987).
[30] F. Cleri and V. Rosato, Phys. Rev. B **48**, 22 (1993).
[31] A. Bryan Edwards, D.J. Tildesley, and N. Binsted, Mol. Phys. **91**, 357 (1997).
[32] A.G. Crooker, M. Donegan, and K.W. Ingle, Philos. Mag. A **41**, 21 (1980).